

# Tuning surface metallicity and ferromagnetism by hydrogen adsorption at the polar ZnO(0001) surface

N. Sanchez, S. Gallego, J. Cerdá, and M. C. Muñoz

*Instituto de Ciencia de Materiales de Madrid, Consejo Superior de Investigaciones Científicas, Cantoblanco, 28049 Madrid, Spain*

(Received 8 September 2009; revised manuscript received 5 February 2010; published 2 March 2010)

Total energy calculations for the adsorption of hydrogen on the polar Zn-ended ZnO(0001) surface predict that a metal-insulator transition and the reversible switch of surface magnetism can be achieved by varying the hydrogen density on the surface. An on top  $H(1 \times 1)$  ordered overlayer with genuine H-Zn chemical bonds is shown to be energetically favorable. The  $H(1 \times 1)$  covered surface is metallic and spin polarized. Lower hydrogen coverages lead to a nonmagnetic insulating surface, with strengthened H-Zn bonds and corrugation of the topmost layers. Our results explain the experimental observation of formation of an ordered  $H(1 \times 1)$  overlayer on the ZnO(0001) surface and its unexpected evolution toward a disordered layer. Furthermore, we identify a mechanism which can contribute to the room-temperature ferromagnetism measured in ZnO thin films and nanoparticles.

DOI: [10.1103/PhysRevB.81.115301](https://doi.org/10.1103/PhysRevB.81.115301)

PACS number(s): 73.20.-r, 73.25.+i, 75.50.Pp, 75.70.Rf

## I. INTRODUCTION

ZnO is a wide band gap semiconductor and one of the most technologically important metal oxides due to its exceptional semiconducting and optical properties.<sup>1</sup> The recently reported high-temperature (HT) ferromagnetism in ZnO-based thin layers and nanostructures<sup>2</sup> turns it additionally into a potential HT prototypical semiconducting ferromagnet, which could be used in magnetoelectric and magnetotransport devices tuning simultaneously charge and spin.<sup>3</sup> However, at present, and despite numerous experimental and theoretical studies, the mechanism behind the HT magnetic order in ZnO is still under debate.<sup>4–7</sup> Many studies on ZnO doped with magnetic ions are in contradiction and even there is not consensus on whether the observed ferromagnetism is intrinsic or due to magnetic clusters, secondary phases or unintentional impurities. Besides, thin films and nanoparticles of undoped ZnO are surprisingly found to exhibit ferromagnetism at HT,<sup>6,8</sup> which has been suggested to be due to surface effects.

In addition, the study of ZnO surfaces has experienced a renewed interest stemming from their relevance in heterogeneous catalysis,<sup>9</sup> and also due to the present ability to grow nanoparticles in a rather large variety of sizes and shapes. For the ZnO polar surfaces, there is also the fundamental stimulus of understanding the stability of the polar terminations of ionic crystals.<sup>10</sup> Particular attention deserves their interaction with H. Although undetectable for most experimental techniques, hydrogen is often present in the environment and its strong reactivity may result in the passivation of polar surfaces with unsaturated dangling bonds. Hence, adsorbed H may drastically alter the properties and even modify the structure of low-dimensional ZnO structures, in which surface phenomena are determinant.

Hydrogen is one of the most abundant impurities in ZnO. Although it has an amphoteric character, isolated hydrogen has always been found to form shallow donor states in bulk ZnO. Therefore, it has been regarded as a source of the unintentional *n*-type conductivity exhibited by ZnO.<sup>11</sup> However, despite the numerous experimental and theoretical stud-

ies, the nature of the *n*-doping remains unclear. While the thermally activated population of the conduction band has been achieved in recent experiments based on reversible hydrogen doping,<sup>12</sup> it has also been shown that the isolated species is not stable at room temperature. Hydrogen migrates through the crystal and forms electrically inactive  $H_2$  molecules, supporting that the hidden species in ZnO is  $H_2$ .<sup>13</sup> Furthermore, some experiments indicate that a high concentration of electron carriers is still present even when hydrogen is removed by thermal treatment at 1100 °C.<sup>14</sup> Hence, native defects cannot be excluded as the origin of the high free electron density. Moreover, interactions between defects lead to a significant reduction in their formation energy, making defects a plausible source of *n*-type conductivity in ZnO.<sup>15</sup>

In recent years, systematic investigations of the different ZnO low-indexed surfaces have been performed, indicating that hydrogen exhibits qualitatively different behavior at the surface than at the bulk.<sup>9</sup> There is agreement in the formation of an ordered hydrogen overlayer on both the nonpolar ZnO ( $10\bar{1}0$ ) and the polar O-ended ZnO ( $000\bar{1}$ ) surfaces. Exposing the ZnO ( $10\bar{1}0$ ) surface to atomic H at low temperature leads to the formation of an ordered overlayer containing two adsorbed H atoms per unit cell, one bonded to O and one to Zn, while adsorption at room temperature results in a metallic surface with an odd number of H atoms per unit cell where H is only bonded to O. Among the polar surfaces, the hydrogen-terminated  $H(1 \times 1)$  O-ZnO ( $000\bar{1}$ ) surface is found to be stable. Nevertheless, the stabilization mechanism needs to be identified, since according to the theoretical analysis the overlayer structure is unstable.<sup>16</sup> On the other hand, the interaction of H atoms with the polar Zn-terminated ZnO(0001) surface is thought to be the weakest among the ZnO surfaces, because the binding energy of ZnH pairs should be considerably weaker than that of OH bonds. An experimental study revealed that, exposing this surface to atomic hydrogen, an ordered  $(1 \times 1)$  overlayer consisting of Zn-hydride species is formed.<sup>17</sup> However, larger exposures to both atomic and molecular hydrogen cause the unexpected instability of the  $H(1 \times 1)$  overlayer, leading to a complete

loss of lateral order which reflects a random distribution of H adatoms.

The aim of this paper is to show that the adsorption of atomic hydrogen on the polar Zn-ZnO(0001) surface gives rise to a tunable system in which it is possible to switch the electronic and magnetic properties by varying the surface H density. As shown below, an on top  $H(1 \times 1)$  ordered overlayer with genuine H-Zn chemical bonds is formed under complete H coverage, surface magnetism and metallicity being its distinct characteristics. The partial desorption of the surface H leads to reinforcement of the H-Zn bonds, corrugation of the surface layer and, more interestingly, the emergence of a spin-paired insulating state. Hence, a metal-insulator transition accompanied by the extinction of the magnetization can be driven by reducing the H density on the surface from 1 monolayer (ML) down to 1/2 ML. Further decrease of the H coverage restores the surface metallicity.

## II. THEORETICAL APPROACH

Our calculations are based on density functional theory employing norm-conserving pseudopotentials and localized numerical atomic orbitals (AOs) as implemented in the SIESTA code.<sup>18</sup> We consider both the local spin-density approximation (LSDA) and the generalized gradient approximation (GGA), with the same basis set and calculation parameters of Ref. 5. Hydrogen is described by a Double Z 1s AO.

Whereas the local-density approximation (LDA) and semilocal GGA approximations for the exchange-correlation potential usually provide structural accuracy, they often fail to describe systems with localized  $d$  electrons. For semiconductors and insulators, the Kohn-Sham single-particle band gap is significantly smaller than the measured quasiparticle band gap. Particularly, the LDA/GGA description of ZnO underestimates the energy gap, and the binding energy of Zn  $d$  states, which consequently are too delocalized and too much hybridized with the Oxygen  $p$ -derived valence states. Hybrid functionals, in which a certain amount of exact non-local Hartree-Fock exchange is added to the LDA/GGA exchange energy, have proved to yield ground-state properties of ZnO in better agreement with experiments.<sup>19</sup> In order to ensure that our conclusions are robust against the choice of the exchange-correlation functional, we have performed additional total energy optimizations with both the Perdew-Burke-Ernzerhof (PBE0) and the screened Heyd-Scuseria-Ernzerhof (HSE) hybrid functionals<sup>20</sup> using the projector augmented wave (PAW) method<sup>21</sup> implemented in the VASP code.<sup>22</sup> We employ similar parameters to those used in Ref. 23, where such functionals were successfully applied to study the defect energetics in ZnO. In our case radial cutoffs of 1.3, 0.9, and 0.4 Å for Zn, O, and H, respectively, are used and a plane-wave cutoff energy of 350 eV. For the hybrid functionals we have used different values of both the amount of exact exchange and the characteristic length, at which the Fock interactions are neglected. The PBE0 functional corresponds to a 0.25 fraction of exact exchange without screening, while the HSE results presented here are obtained including a 0.35 fraction of exact exchange at a range

of 0.2 Å<sup>-1</sup>. As shown below, despite the better description of both the ZnO band gap and the energy and localization of Zn  $d$  states using hybrid functionals, the electronic structure at the valence band edge is analogous for the different exchange correlation functionals. This is the important energy window containing the hydrogen induced states for the H covered ZnO surfaces under study.

The surfaces of intrinsic—dopant free—ZnO crystals and those covered by neutral hydrogen adlayers are modeled by periodically repeated slabs containing between 15 and 17 atomic planes, separated by a vacuum region of at least 20 Å. Bulk-like behavior is always attained at the innermost central layers. We calculate both symmetric and asymmetric slabs about the middle plane, though we are always subject to the lack of inversion symmetry of the wurtzite structure. Hydrogen induced effects result to be independent of the symmetric or asymmetric structure of the slab. We use  $(1 \times 1)$  and  $(2 \times 2)$  two-dimensional (2D) unit cells to model the surfaces with adsorbed hydrogen. All the atomic positions are allowed to relax until the forces on the atoms are less than 0.03 eV/Å. Brillouin zone (BZ) integrations have been performed on a  $12 \times 12 \times 1$  Monkhorst-Pack supercell ( $12 \times 12 \times 8$  for bulk structures). Careful convergence in the  $k$ -mesh and the inclusion of relaxations are essential in order to accurately describe the adsorption states and magnetism.

The H-Zn bonding properties are analyzed mainly in terms of density of states projected (PDOS) onto the surface atoms. They have been evaluated both for the 2D slabs employed for the density functional theory optimizations as well as for semi-infinite geometries—i.e., surface plus bulk—following the prescription of Ref. 24. Additionally, we have performed Mulliken and crystal orbital overlap population (COOP) analysis.<sup>25</sup> These quantities give information on the electronic charge at the atomic sites and on the charge shared by any pair of atoms, respectively. Hereafter, we will use the term charge referring to these populations, despite there is no strict equivalence between them, e.g., the Mulliken populations are basis set dependent. Nevertheless, their trends with the H coverage provide a comprehensive representation of the charge redistribution occurring at the surface.

## III. HYDROGEN ADSORPTION

### A. Ordered $(1 \times 1)$ hydrogen overlayer

For 1 ML coverage, the stable adsorption site of H was determined to be atop the Zn atoms after exhaustive minimization considering several surface and subsurface positions, including *fcc* and *hcp* hollow, bridge and off-symmetric sites. We present in Fig. 1 the PDOS onto the outermost layers for the bare and H covered surface, both using LDA and the HSE functional. For comparison, the PDOS corresponding to a substitutional H atom at an oxygen site in bulk ZnO—multicenter bonds configuration (MBC)<sup>11</sup>—is also shown. As expected, the HSE functional gives a better description of the band gap and increases the localization of the Zn  $d$  states. The calculated gaps using LDA and HSE for bulk ZnO are 0.80 and 3.45 eV, respectively, compared to the experimental value of 3.40 eV.<sup>26</sup> The results obtained with

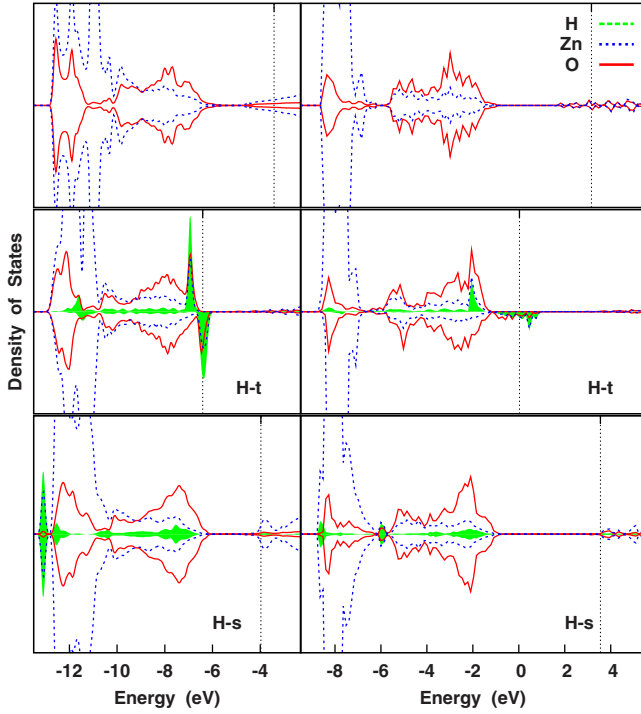


FIG. 1. (Color online) PDOS on the H (filled curve) and outermost Zn and O atoms of the Zn-Zn(0001) surface either bare (top panels) or covered by 1 ML of H (middle panels). The left (right) column corresponds to LDA (HSE) calculations. At the bottom panels we provide the PDOS on the H and neighboring Zn and O atoms for bulk ZnO with a H impurity in the MBC.

GGA, not shown in Fig. 1, are analogous to those of LDA. Further, the HSE and PBE0 yield similar band gaps and Zn *d*-states localizations despite the long-range screening of the Hartree-Fock exchange in the former. Therefore, the physical picture provided by calculations performed with different approximations for the exchange-correlation potential is equivalent, supporting their accuracy. The clean surface exhibits the well-known metallic character, with the occupied surface states (SSs), arising from the unsaturated dangling bonds of surface Zn, placed at the bottom of the conduction band (CB).<sup>27</sup> An adsorbed H interacts with a surface Zn atom and forms a strong Zn-H bond. The hybridized bonding state is located at the valence band (VB) edge and is partially filled, so the Fermi level lies in the H derived states and the surface is metallic and *hole* doped. Therefore, the adsorption of hydrogen changes the position of the Fermi level ( $E_F$ ) at the surface layer with respect to the band edges.  $E_F$  shifts from the CB edge for the Zn bare surface to the VB edge for the hydrogen covered surface. Conversely, H in the bulk MBC interacts with the unsaturated dangling bonds of the four surrounding Zn atoms to form a bonding state located deep below the VB and an antibonding state lying in the CB of ZnO. The electron, which would occupy the antibonding state, is transferred to the CB minimum. Thus, the complex composed of the hydrogen and the four nearest-neighbor Zn atoms acts as a shallow donor.<sup>11</sup> Note that while in the hydrogen covered surface all surface Zn atoms are bonded to hydrogen, in the MBC there is an isolated hydrogen impurity in a ZnO bulk crystal.

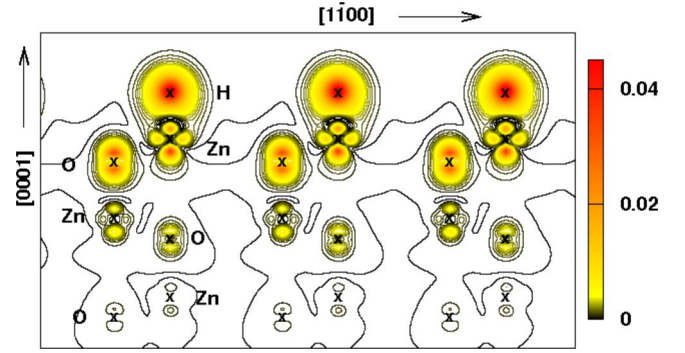


FIG. 2. (Color online) Side view of the spin density distribution of the ZnO(0001) surface covered by 1 ML H, along a plane containing the Zn-O bonds. The contour lines correspond to steps of  $5 \times 10^4$  electrons.

A distinct characteristic of the H covered surface in the atop geometry is the spin-polarization of the bands. It is not restricted to the H layer, but extends into the ZnO subsurface leading to a net magnetization of the surface region. This is clearly seen in Fig. 2, in which up to four ZnO atomic planes present spin-polarization. The magnetic moments at the H, Zn and O layers are 0.29, 0.09 and 0.09  $\mu_B$ /atom, respectively, being 0.50  $\mu_B$  the total magnetization induced by a hydrogen. The magnetic energy gain, defined as the difference between the total energy of the magnetic ground state and that corresponding to a non-spin-polarized state, is around 70 meV per unit cell containing just a hydrogen atom. Similar values are obtained in the HSE calculation, the total magnetization differing in less than 10%. Summarizing, H adsorption at the ML coverage gives rise to a hole-doped metallic surface with the Fermi level at the outermost layers pinned below the VB maximum at the H-derived bands. Furthermore, there is a magnetization of the surface with a net magnetic moment of around 0.5  $\mu_B$  per hydrogen atom.

### B. Partial hydrogen coverage

In order to understand the emergence of the spin polarization when going from the bare Zn surface to the complete H overlayer, we have modeled partial hydrogen coverages of 3/4, 1/2, and 1/4 MLs with LDA. The corresponding geometric and electronic structures are displayed in Fig. 3 and further details are given in Table I. The adsorption of H creates low dispersion states at the top of the VB, which are spin-split for 1 ML coverage, with only one spin component completely filled. Furthermore, the spin-split states start to merge for lower coverages until they become degenerate for 1/2 ML of H. The loss of spin polarization is accompanied by a metal to insulator transition of the surface. Thus, while at 3/4 ML the surface is still ferromagnetic and metallic, for coverage of 1/2 ML the ground state corresponds to a nonmagnetic insulator with the Fermi level above the hydrogen derived band. Further decrease of the hydrogen coverage results in partial occupation of the CB states due to the increased number of unsaturated Zn dangling bonds, restoring the surface metallicity. Therefore, our results reveal that the H covered Zn-ZnO (0001) surface is a novel system, in



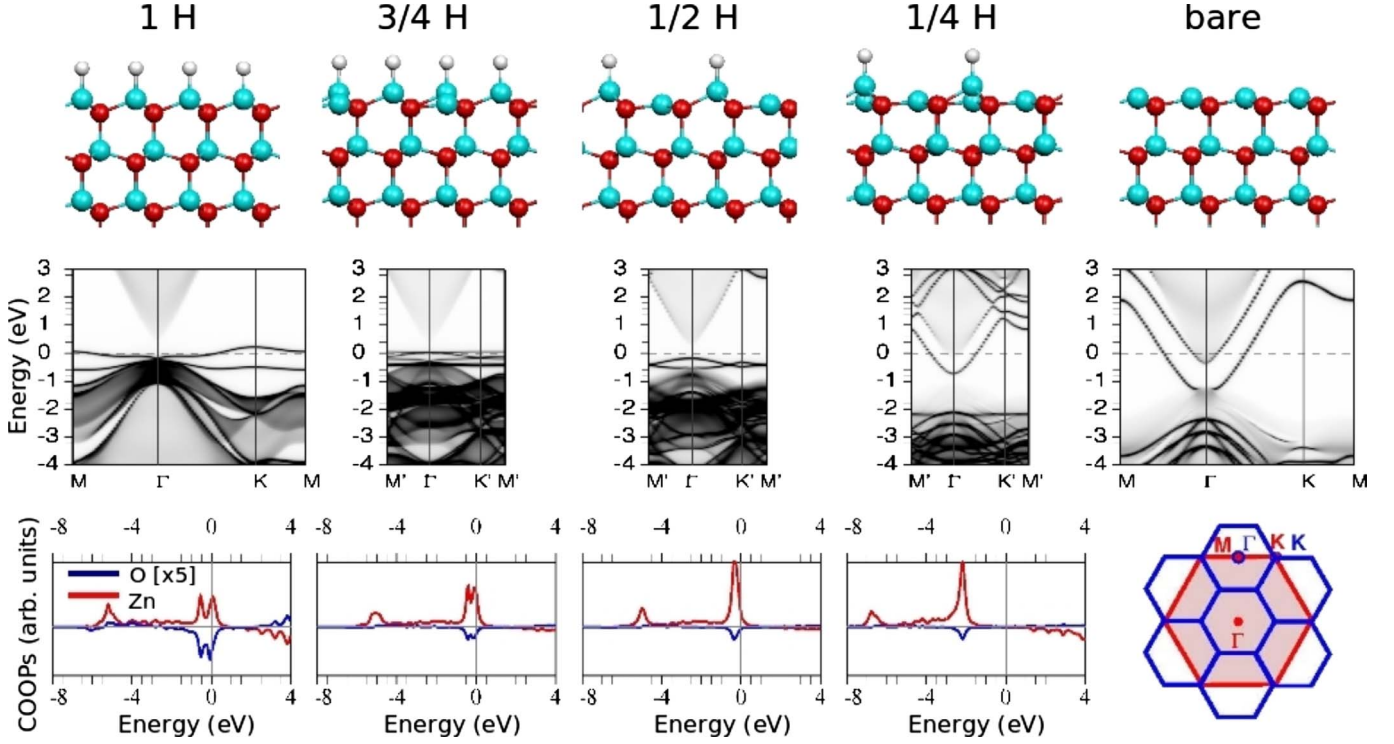


FIG. 3. (Color online) (Top) Side views of the ZnO(0001) surface for decreasing H coverage from left to right. Oxygen, Zn and H atoms are colored in red (black), blue (gray), and white, respectively. Below each sketch we provide for each case the corresponding: (middle) PDOS projected on the first surface layers calculated for the semi-infinite crystal and resolved in  $k$ -space (Ref. 24)—the BZ for the  $(1 \times 1)$  and  $(2 \times 2)$  2D cells is depicted at the right of the bottom panel; (bottom) H-Zn and H-O (magnified by a factor of 5) COOPs.

which a metal to insulator transition can be tuned by varying the H-coverage back and forth. Even more, by modifying the hydrogen density reversible switch of surface magnetism can be achieved.

A deeper insight about this remarkable phenomenon can be obtained regarding the nature of the bonds, see Table I. In all cases, the H-Zn bond length, which coincides with the interlayer distance for the on top adsorption site, is significantly shorter than at the bulk ( $\sim 2$  Å in the MBC), a hint of the formation of genuine and stronger chemical bonds at the surface. Furthermore, the bond length reduces as the H coverage diminishes, evidencing a reinforcement of the H-Zn bonds. This bond strengthening is consistent with the variation of the Mulliken populations and the corresponding COOPs displayed in the lower panel of Fig. 3. The electronic

charge localized at both the H and the Zn increases as the H coverage reduces, indicating that a larger amount of charge is shared between the two atoms. The COOPs confirm this scenario; their positive value corresponds to bonding states,<sup>25</sup> which are progressively filled as the H coverage reduces. Noticeably, hydrogen also interacts with the O in the subsurface layer forming an antibonding state. However, the Mulliken population of Oxygen atoms remains almost unchanged and close to the bulk values.

The reinforcement of the H-Zn bonds can be understood regarding the atomic structures in Fig. 3 and Table I. For the clean surface we find a contraction of the first double layer spacing,  $d_{\text{Zn-O}}$ , in agreement with previous calculations.<sup>27</sup> Contrary, the surface completely covered with H exhibits a slightly expanded Zn-O distance. For partial H coverages the

TABLE I. H-related surface energy ( $E_{\text{surf}}$ , in eV), interlayer distances ( $d$ , in Å), and total Mulliken populations ( $Q$ ) of the surface atoms for the Zn-ended ZnO(0001) surface covered by different amounts of H (from 1 to  $1/4$  ML of H) and bare. For partial coverages, the inequivalent Zn surface atoms are distinguished as  $\text{Zn}^{\text{H}}$ , bonded to H, and  $\text{Zn}^{\text{DB}}$ , with a dangling bond. As a reference, the last column provides values for the undoped bulk ZnO.

	1 H	3/4 H	1/2 H	1/4 H	Bare	Bulk
$d_{\text{H-Zn}}$	1.62	1.60	1.57	1.56		
$d_{\text{Zn}^{\text{H}}\text{-O}}/d_{\text{Zn}^{\text{DB}}\text{-O}}$	0.71	0.78/0.21	0.91/0.20	1.02/0.14	0.39	0.61
$Q_{\text{H}}$	1.09	1.12	1.17	1.21		
$Q_{\text{Zn}^{\text{H}}}/Q_{\text{Zn}^{\text{DB}}}$	11.36	11.38/11.25	11.42/11.24	11.45/11.27	11.37	11.23
$E_{\text{surf}}$	-1.53	-1.86	-2.51	-3.22		

surface Zn atoms become inequivalent, leading to two different Zn-O interlayer distances and a large corrugation of the Zn plane: Zn atoms bonded to H experience an outward relaxation while the unbonded ones show an inward relaxation even stronger than that at the bare surface, becoming almost coplanar with the oxygen plane. For deeper layers little relaxation is found. There is a strong correlation between the Zn-O interlayer distance and the redistribution of charge: Zn atoms bonded to H—large  $d_{\text{Zn-O}}$ —show an increase in their Mulliken populations, while those not bonded—small  $d_{\text{Zn-O}}$ —lose charge approaching the bulk values.

The energies provided in Table I for the H covered surfaces also support the formation of strong bonds with a significant covalent character. They are calculated as the difference between the total energy of the relaxed slab and those of the relaxed isolated ZnO and hydrogen slabs. Their negative values indicate that the chemisorption of H on the Zn(0001) surface is favorable. In fact, at a hydrogen density of 1/2 ML the adsorption is exothermic. The surface energy exceeds by 140 meV the formation of the  $\text{H}_2$  molecule in the gas phase, 2.37 eV/H, making adsorbed hydrogen highly stable against desorption. In addition, there is a net reduction of the surface energy for all H coverages with respect to the bare surface. This is specially significant for partial H coverages, where the existence of inequivalent Zn sites allows for the corrugation of the Zn layer and the subsequent decrease of surface energy.

As a final remark, the Zn-ZnO(0001) surface may undertake a triangularly shaped reconstruction under specific growth conditions.<sup>28</sup> We have investigated the effect of such reconstruction through calculations of stepped surfaces, and the general conclusions are analogous to those presented here for the unreconstructed surface, although strong O-H bonds are also formed at step edges.

#### IV. DISCUSSION AND CONCLUSIONS

Our findings consistently explain experimental results about the formation and structure of hydrogen adlayers on the Zn-ZnO(0001) surface. He-atom scattering revealed not only the formation of a  $\text{H}(1 \times 1)$  ordered overlayer, but also the loss of surface order under prolonged hydrogen exposures.<sup>17</sup> As shown above, partial H adsorption is energetically more favorable than the bare and fully covered surfaces, which could explain the experimentally observed instability of the  $(1 \times 1)$  ordered overlayer and its evolution toward less densely packed disordered structures. In addition, the formation of such disordered and highly corrugated terminations provides the clue to understand the enhancement of the chemical reactivity of surfaces previously exposed to H with respect to the pristine ones. Also the almost coplanar positions of the Zn and O atoms in the bare regions of the partially H covered surface can account for the observed surface restructuring and for the oxygen signature detected in the x-ray photoemission spectra (XPS).<sup>17</sup>

Unfortunately, to our knowledge information about the electronic properties of the hydrogen covered surface is not available. Although control of the graphene properties by reversible hydrogenation has been recently achieved,<sup>29</sup> for

the Zn-ZnO(0001) surface further experimental research is deserved to confirm our predictions about the possibility to reversibly control the conductivity and tune the surface magnetism. In this sense, it is interesting to evaluate the implications of the unintentional *n*-type conductivity exhibited by ZnO samples, pinning the Fermi level close to or in the CB minimum. As stated above, the clean Zn polar (0001) face shows a charge polarization arising from the lack of inversion symmetry of the wurtzite structure and the partly ionic nature of the Zn-O bond. The electrons in the CB are bound to the surface region and then, for an intrinsic—dopant free—ZnO crystal as modeled by us, a downward band bending is present near the surface. Adsorption of H passivates the Zn dangling bonds creating holes in the VB and the energy bands bend strongly upward. Under *n*-type conditions, free electrons will likely move toward the hydrogen covered surface in an attempt to compensate its positive polarization. Thus, an electron accumulation region will be formed adjacent to the H-Zn surface, contributing to reduce the number of hydrogen induced VB holes bound to the surface region. However, the number of free electrons in the accumulation layer will be insufficient to compensate the positive surface sheet of holes. First, the surface density of holes is large, approximately half hole per surface unit cell,<sup>30</sup> i.e., around  $10^{14}$  hole  $\text{cm}^{-2}$ . In addition, in most common cases, the carriers can still be bound to the ionized defect center by the Coulomb interaction in a hydrogenic effective-mass state, which lowers the effective concentration of free carriers hindering the hole compensation. Then, although *n*-doping will compensate some of the surface VB holes, it is unlikely that it would completely destroy the surface metallicity induced by the hydrogen adsorption.

Finally, an additional important conclusion can be extracted with respect to the HT ferromagnetism measured in ZnO-based thin layers and nanoparticles, both undoped and doped with magnetic impurities. Various experimental investigations exclude the magnetic elements as the origin of the HT ferromagnetism in ZnO nanoparticles and nanostructured granular films doped with magnetic elements.<sup>31</sup> Moreover, as has been recently revealed in a detailed analysis of the extended experimental bibliography about magnetism on pure ZnO and Mn-doped ZnO, grain boundaries and related vacancies are likely to be the intrinsic source of HT ferromagnetism.<sup>32</sup> HT ferromagnetism has also been reported in ZnO doped with nonmagnetic atoms and in undoped ZnO nanostructures, and recent experimental studies have shown that the occurrence of surface ferromagnetism is a universal characteristic of oxide nanoparticles.<sup>33</sup> This scenario corroborates our previous predictions of surface magnetism at the O-terminated surface of ionic oxides and in particular of ZnO, due to the presence of *p* holes in the valence band of the oxide.<sup>5,34</sup> A step forward, our present results strongly suggest that unintentionally adsorbed hydrogen may also take active part in the observed magnetism, particularly for undoped ZnO nanocrystals. Since HT ferromagnetism has been observed to vary with the oxygen partial pressure, its existence has been associated to oxygen vacancies. However, calculations as well as careful experiments indicate that oxygen vacancies cannot be a source of magnetism, but instead it may develop from unsaturated oxygen either due to Zn

vacancies or to O-terminated surfaces.<sup>5–7,35</sup> Adsorbed hydrogen is sensitive to the oxygen partial pressure, since the probability of formation of HO complexes increases with the oxygen chemical potential, leading to the subsequent extinction of the magnetism reported here. Moreover, the hydrogen electron spin has been measured in  $\text{In}_2\text{O}_3$  when hydrogen acts as an oxygen vacancy passivating center, demonstrating the ability of H to be spin polarized.<sup>36</sup>

In conclusion, our first-principles calculations show that atomic hydrogen adsorbs on the Zn-ZnO(0001) polar surface atop the Zn atoms, forming strong H-Zn bonds and leading to a metallic, hole-doped surface with a net magnetic moment. As the H coverage diminishes, there is a reinforcement of the remaining H-Zn bonds accompanied by the removal of the valence band holes and the subsequent extinction of magnetism. We predict that controlling the hy-

drogen coverage can serve to transform the conductive polar surface into an insulator and hence to tune a metal-insulator transition and to achieve reversible switch of surface magnetism.

## ACKNOWLEDGMENTS

We are indebted to P. Esquinazi and N. García for fruitful discussions. We also acknowledge the invaluable support of C. Franchini and J. Häfner in the calculations using hybrid functionals. This work was supported by the Spanish Ministry of Science and Technology (Grants No. MAT2006-05122 and No. MAT2007-66719-C03-2). The resources of the Supercomputing Centre of Galicia (CESGA) were used for the calculations.

- <sup>1</sup>Ü. Özgür, Ya. I. Alivov, C. Liu, A. Teke, M. A. Reshchikov, S. Doğan, V. Avrutin, S.-J. Cho, and H. Morkoç, *J. Appl. Phys.* **98**, 041301 (2005).
- <sup>2</sup>K. Ueda, H. Tabedo, and T. Kawai, *Appl. Phys. Lett.* **79**, 988 (2001).
- <sup>3</sup>D. D. Awschalom and M. E. Flatté, *Nat. Phys.* **3**, 153 (2007).
- <sup>4</sup>S. A. Chambers and B. Gallagher, *New J. Phys.* **10**, 055004 (2008).
- <sup>5</sup>N. Sanchez, S. Gallego, and M. C. Muñoz, *Phys. Rev. Lett.* **101**, 067206 (2008).
- <sup>6</sup>A. Sundaresan, R. Bhargavi, N. Rangarajan, U. Siddesh, and C. N. R. Rao, *Phys. Rev. B* **74**, 161306(R) (2006).
- <sup>7</sup>Q. Xu, H. Schmidt, S. Zhou, K. Potzger, M. Helm, H. Hochmuth, M. Lorenz, A. Setzer, P. Esquinazi, C. Meinecke, and M. Grundmann, *Appl. Phys. Lett.* **92**, 082508 (2008).
- <sup>8</sup>M. A. Garcia, J. M. Merino, E. Fernández Pinel, A. Quesada, J. de la Venta, M. L. Ruíz González, G. R. Castro, P. Crespo, J. Llopis, J. M. González-Calbet, and A. Hernando, *Nano Lett.* **7**, 1489 (2007).
- <sup>9</sup>C. Wöll, *Prog. Surf. Sci.* **82**, 55 (2007) and references therein.
- <sup>10</sup>V. Staemmler, K. Fink, B. Meyer, D. Marx, M. Kunat, S. G. Girol, U. Burghaus, and Ch. Wöll, *Phys. Rev. Lett.* **90**, 106102 (2003).
- <sup>11</sup>C. G. Van de Walle, *Phys. Rev. Lett.* **85**, 1012 (2000); A. Janotti and C. G. Van de Walle, *Nature Mater.* **6**, 44 (2007).
- <sup>12</sup>H. Qiu, B. Meyer, Y. Wang, and C. Wöll, *Phys. Rev. Lett.* **101**, 236401 (2008).
- <sup>13</sup>E. V. Lavrov, F. Herklotz, and J. Weber, *Phys. Rev. Lett.* **102**, 185502 (2009); *Phys. Rev. B* **79**, 165210 (2009).
- <sup>14</sup>L. E. Halliburton, N. C. Giles, N. Y. Garces, Ming Luo, Chun-chuan Xu, Lihai Bai, and L. A. Boatner, *Appl. Phys. Lett.* **87**, 172108 (2005).
- <sup>15</sup>Y.-S. Kim and C. H. Park, *Phys. Rev. Lett.* **102**, 086403 (2009).
- <sup>16</sup>B. Meyer, *Phys. Rev. B* **69**, 045416 (2004).
- <sup>17</sup>T. Becker, S. Hövel, M. Kunat, C. Boas, U. Burghaus, and C. Wöll, *Surf. Sci.* **486**, L502 (2001); **511**, 463 (2002).
- <sup>18</sup>J. M. Soler, E. Artacho, J. D. Gale, A. García, J. Junquera, P. Ordejón, and D. Sánchez-Portal, *J. Phys.: Condens. Matter* **14**, 2745 (2002).
- <sup>19</sup>J. Wróbel, K. J. Kurzydłowski, K. Hummer, G. Kresse, and J. Piechota, *Phys. Rev. B* **80**, 155124 (2009).
- <sup>20</sup>J. Paier, M. Marsman, K. Hummer, G. Kresse, I. C. Gerber, and J. G. Ángyán, *J. Chem. Phys.* **124**, 154709 (2006) and references therein.
- <sup>21</sup>G. Kresse and D. Joubert, *Phys. Rev. B* **59**, 1758 (1999).
- <sup>22</sup>G. Kresse and J. Hafner, *Phys. Rev. B* **47**, 558(R) (1993); G. Kresse and J. Furthmüller, *ibid.* **54**, 11169 (1996).
- <sup>23</sup>F. Oba, A. Togo, I. Tanaka, J. Paier, and G. Kresse, *Phys. Rev. B* **77**, 245202 (2008).
- <sup>24</sup>C. Rogero, C. Koitzsch, M. E. González, P. Aebi, J. Cerdá, and J. A. Martín-Gago, *Phys. Rev. B* **69**, 045312 (2004).
- <sup>25</sup>J. I. Beltrán, S. Gallego, J. Cerdá, J. S. Moya, and M. C. Muñoz, *Phys. Rev. B* **68**, 075401 (2003).
- <sup>26</sup>K.-H. Hellwege and O. Madelung, *Numerical Data and Functional Relationships in Science and Technology*, Landolt-Börnstein, New Series, Group III (Springer, New York, 1982).
- <sup>27</sup>G. Kresse, O. Dulub, and U. Diebold, *Phys. Rev. B* **68**, 245409 (2003).
- <sup>28</sup>O. Dulub, U. Diebold, and G. Kresse, *Phys. Rev. Lett.* **90**, 016102 (2003).
- <sup>29</sup>D. C. Elias, R. R. Nair, T. M. G. Mohiuddin, S. V. Morozov, P. Blake, M. P. Halsall, A. C. Ferrari, D. W. Boukhvalov, M. I. Katsnelson, A. K. Geim, and K. S. Novoselov, *Science* **323**, 610 (2009).
- <sup>30</sup>The hybrid H-Zn orbital is occupied by one and a half electrons, one from the hydrogen and half from the Zn dangling bond.
- <sup>31</sup>Z. H. Zhang, X. Wang, J. B. Xu, S. Muller, C. Ronning, and Q. Li, *Nat. Nanotechnol.* **4**, 523 (2009).
- <sup>32</sup>B. B. Straumal, A. A. Mazilkin, S. G. Protasova, A. A. Myatiev, P. B. Straumal, G. Schütz, P. A. van Aken, E. Goering, and B. Baretzky, *Phys. Rev. B* **79**, 205206 (2009).
- <sup>33</sup>A. Sundaresan and C. N. R. Rao, *Solid State Commun.* **149**, 1197 (2009).
- <sup>34</sup>S. Gallego, J. I. Beltrán, J. Cerdá, and M. C. Muñoz, *J. Phys.: Condens. Matter* **17**, L451 (2005).
- <sup>35</sup>H. Peng, H. J. Xiang, S.-H. Wei, S.-S. Li, J.-B. Xia, and J. Li, *Phys. Rev. Lett.* **102**, 017201 (2009).
- <sup>36</sup>M. Kumar, R. Chatterjee, S. Milikisiyants, A. Kanjilal, M. Voelskow, D. Grambole, K. V. Lakshmi, and J. P. Singh, *Appl. Phys. Lett.* **95**, 013102 (2009).